International Journal of GEOMATE, Nov., 2017, Vol.13, Issue 39, pp.124-131
Geotec., Const. Mat. & Env., ISSN:2186-2990, Japan, DOI: https://doi.org/10.21660/2017.39.98548

FIELD MEASUREMENT AND NUMERICAL MODELING OF TIDAL CURRENT IN LARANTUKA STRAIT FOR RENEWABLE ENERGY UTILIZATION

*Harman Ajiwibowo[1], Kanisius Sagari Lodiwa[2], Munawir Bintang Pratama[3], and Andojo Wurjanto[4]

[1] Faculty of Civil and Environmental Engineering, Institut Teknologi Bandung, Indonesia

*Corresponding Author, Received: 17 June 2017, Revised: 10 July 2017, Accepted: 2 Aug 2017

ABSTRACT: The amount of electricity consumed is growing rapidly, along with population growth and technological development. Meanwhile, Indonesia's energy supply is predominantly supported by non-renewable sources, so an approach to renewable energy is urgently needed. This study uses a numerical model to determine the potency of tidal current power at Larantuka Strait, East Nusa Tenggara Province, Indonesia. The output of the study is the electricity generated with a conversion device at several locations. The numerical model is generated using MIKE 3. In order to validate the numerical model, field measurements are conducted to obtain the detailed bathymetry, tidal surface elevation, and tidal current velocity data. The numerical model shows good agreement with the field measurement data; the average errors of tidal surface elevation and tidal current velocity are 4.04 and 9.79%, respectively. Furthermore, the tidal current model is analyzed and two potential sites are found at the narrowest part of the strait. The generated power is calculated for a D10 Sabella turbine. The calculation shows that the amounts of power generated are 522.972 and 324.12 MWh for the two sites, respectively, in 2014. The study shows that Larantuka Strait is very promising and suitable as a site for a tidal current power plant with its tidal current and water depth. A detailed analysis, including financial, navigation, and environmental studies, needs to be conducted to present the feasibility of the realization.

Keywords: Numerical modeling, Tidal current, Ocean renewable energy, Larantuka Strait, Indonesia.

1. INTRODUCTION

In recent times, human requirements have grown rapidly in both developed and developing countries across the globe. The increase in the world's population and the importance of digital life have become major challenges with their impact on the requirement to provide electricity. Meanwhile, with the currently available technology in Indonesia, increasing energy production is equivalent to increasing carbon dioxide emissions to the environment.

Therefore, exploration of renewable energy utilization is required to solve the energy problem. Renewable energy from the ocean is one of the most promising energy sources in Indonesia, whose area consists of approximately 70% water. Tidal current energy is the most favorable ocean renewable energy source according to the physical oceanography characteristics in Indonesia.

Several studies related to tidal current energy have been conducted across the world, such as in Scotland [1], France [2], Canada [3], the USA [4], Brazil [5], China [6], Taiwan [7], Korea [8], Japan [9], and India [10]. There have also been some studies of tidal energy in Indonesia. The studies show that there are a total of seven potential sites for extracting electricity from tidal current energy in Indonesia [11]–[13]. A study by Orhan et al. [12] stated that Larantuka Strait has tremendous tidal energy sources with some specific locations having power density of 6 kW/m^2. The objective of this study is to provide a more detailed analysis of energy production in Larantuka Strait. This study is performed with modeling tools (MIKE 3) and determines the specific extracted energy in energy consumption units.

2. STUDY LOCATION

Larantuka Strait is located between the eastern part of Flores Island and Adonara Island in East Nusa Tenggara Province in Indonesia. Larantuka Strait links Banda Sea and Savu Sea from north to south with a tapered channel from both directions. A general view of Larantuka Strait is given in Fig. 1 (b) and the specific location of Larantuka Strait is shown with a red box.

Larantuka Strait is about 8 km in length. The north and south inlets of Larantuka Strait are both around 4.5 km wide. Meanwhile, at the narrowest part, the width of the strait is approximately 600 m and the depth is 20 m.

The high-velocity tidal current in Larantuka Strait is formed by mass transport from the Banda

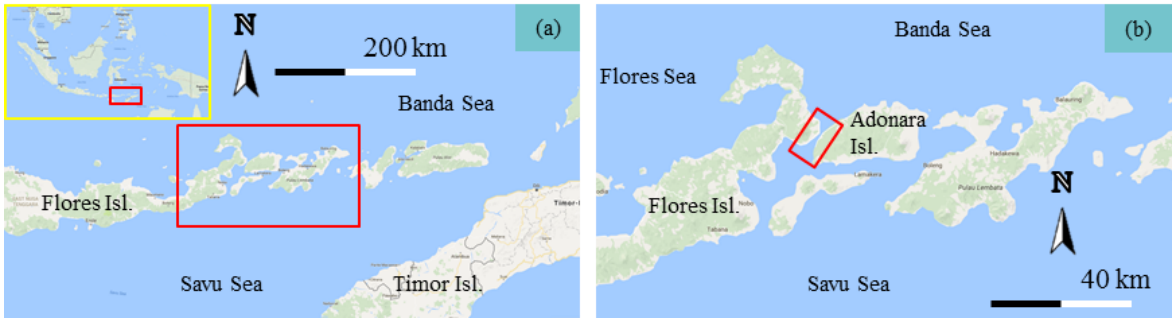

Fig.1 Location of (a) East Nusa Tenggara and (b) Larantuka Strait

Sea to the Savu Sea and vice versa. The main cause of this high velocity is the significant narrowing of the strait, and this effect is intensified by the Indonesian Through flow. The tidal range and tidal current peak velocity in Larantuka Strait are 3 m and 3 to 4 m/s, respectively [12].

3. SCOPE

This study's objectives are to provide a valid hydrodynamic model of Larantuka Strait and to calculate the converted tidal current power. In attempting to develop the model, it is important to validate it with field measurement data. The produced model is used to determine potential sites with a high tidal current velocity to be converted into electricity.

This study contains several integrated activities including data collection, field measurement, hydrodynamic modeling, tidal current model analysis, potential site analysis, and calculation of the converted power.

4. FIELD MEASUREMENTS

Field measurements are conducted to determine several physical conditions of Larantuka Strait. Three field measurement surveys are conducted: bathymetry, surface elevation, and tidal current velocity. The area of the bathymetry survey and the locations of the surface elevation and tidal current velocity surveys are shown in Fig. 2.

4.1 Bathymetry

The bathymetric survey equipment comprises a transducer and a GPS-Echosounder. The bathymetric survey is conducted to provide a base map of an area of 3 × 5 km^2 of Larantuka Strait located at the UTM coordinate of 51 South region. The area of the bathymetric survey is shown in Fig. 2 as a dotted black line.

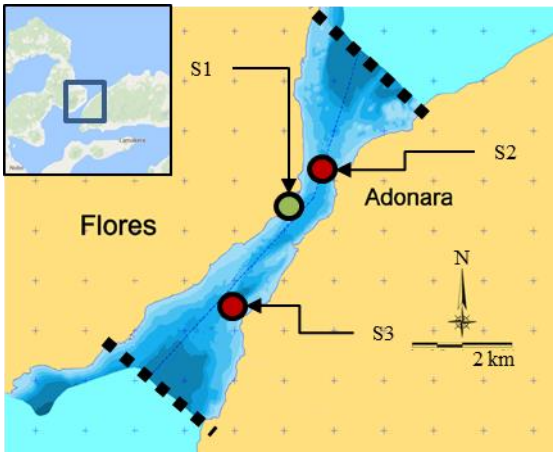

Fig.2 Field measurement location

4.2 Surface Elevation

The tidal survey is carried out by observation on peilschaal in Paloh Beach, Larantuka. The location is shown in Fig. 2 as S1 (502,060 m E, 9,080,420 m S). The location is chosen as it is calm and the depth is able to present both high and low water conditions. The surface elevation data are recorded every hour for 15 days (half-moon cycle), from November 21, 2013 to December 4, 2014. The water surface elevation survey shows that the tidal range is 2.6 m. It is also found that the tidal characteristic in Bangka Strait is mixed, being mainly semi-diurnal.

4.3 Tidal Current

The tidal current velocity is measured using an ADCP Argonaut-XR with a 0.75-MHz autonomous multi-cell system specification. The survey is conducted at S2 (503,052 m E, 9,081,710 m S) and S3 (501,101 m E, 9,078,492 m S), as shown in Fig. 2. The ADCP height is 0.8 m above the seabed and located at the depth of 20 m. The acquired data are collected from 10 layers in order to have detailed velocity data so that good accuracy can be obtained

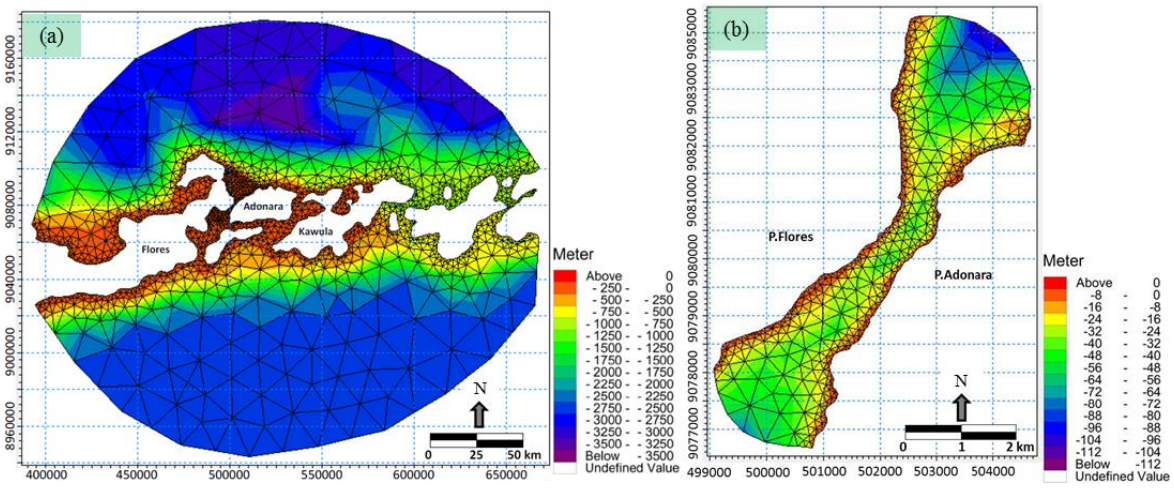

Fig.3 The mesh of the (a) global model and the (b) local model

for the model validation. Layer 10 is located nearest to the water's surface. Meanwhile, layer 1 is directly above the ADCP.

The measured tidal current velocity at S2 ranges from 0.4 to 194.3 cm/s. Meanwhile, in S3 the range is 0 to 286 cm/s. The lowest and highest tidal current velocities are found to occur at layers 1 and 10, respectively.

The direction of the tidal current velocity is also known to be predominantly to the northwest when transitioning from flood to ebb. Meanwhile, the flow direction is to the southeast when the condition changes from ebb to flood.

5. NUMERICAL MODEL

A numerical model is developed to provide some particular parameter distributions at several points at any particular time. Several previous studies have also carried out modeling using various tools, such as Delft3D [14], FVCOM (Finite Volume Coastal Ocean Model) [1], ROMS (Regional Ocean Model System) [4], and MIKE [6].

This study uses MIKE 3 with a personal license. MIKE 3 has become one of the leading tools in multipurpose hydrodynamic modeling in the world. It has also been used for a lot of research, such as modeling storm surges [15], river processes [16], environmental quality [17], tsunamis [18], and the power potency of a tidal current [6].

5.1 Governing Equations

The three-dimensional hydrodynamic model with sigma coordinates is developed using MIKE 3. The model solves the three-dimensional incompressible Reynolds-averaged Navier-Stokes (RANS) equations using the Boussinesq and hydrostatic pressure assumptions with the finite element method [19].

Equation (1) shows the local continuity equation for the model, which is performed in Cartesian and sigma coordinates. The two horizontal momentum equations for the x- and y- components are presented in Eq. (2) and Eq. (3).

$$\frac{\partial h}{\partial t}+\frac{\partial hu}{\partial x'}+\frac{\partial hv}{\partial y'}+\frac{\partial h\omega}{\partial \sigma}=hS \tag{1}$$

$$\frac{\partial hu}{\partial t}+\frac{\partial hu^2}{\partial x'}+\frac{\partial hvu}{\partial y'}+\frac{\partial h\omega u}{\partial \sigma}=fvh-gh\frac{\partial \eta}{\partial x'}$$
$$-\frac{h}{\rho_0}\frac{\partial p_a}{\partial x'}-\frac{hg}{\rho_0}\int_z^n\frac{\partial \rho}{\partial x}dz-\frac{1}{\rho_o}\left(\frac{\partial s_{xx}}{\partial x}+\frac{\partial s_{xy}}{\partial y}\right)$$
$$+hF_u+\frac{\partial}{\partial \sigma}\left(\frac{v_v}{h}\frac{\partial u}{\partial \sigma}\right)+hu_sS \tag{2}$$

$$\frac{\partial hv}{\partial t}+\frac{\partial huv}{\partial x'}+\frac{\partial hv^2}{\partial y'}+\frac{\partial h\omega v}{\partial \sigma}=-fuh-gh\frac{\partial \eta}{\partial y'}$$
$$-\frac{h}{\rho_0}\frac{\partial p_a}{\partial y'}-\frac{hg}{\rho_0}\int_z^n\frac{\partial \rho}{\partial y}dz-\frac{1}{\rho_o}\left(\frac{\partial s_{yx}}{\partial x}+\frac{\partial s_{yy}}{\partial y}\right)$$
$$+hF_v+\frac{\partial}{\partial \sigma}\left(\frac{v_v}{h}\frac{\partial v}{\partial \sigma}\right)+hv_sS \tag{3}$$

where t is the time; x', y', and σ are the modified Cartesian coordinates; u, v, and w are the velocities in the x', y', and σ axis; h is the total water depth; η is the water level from MSL; f is the Coriolis parameters; g is the gravitational acceleration; p_a is the atmospheric pressure; ρ_0 is the fluid density; v_s is the vertical turbulent viscosity; s_{xx}, s_{xy}, s_{yx}, and s_{yy} are the radiation stress components; S is the magnitude of

point source discharge; Lastly, u_s and v_s are the velocities of the discharge.

5.2 Model Setup

Numerical modeling is carried out in two stages using a regional model and a local model, both of which are executed in Cartesian and sigma coordinates. The global model covers Savu Sea, Banda Sea, and Flores Sea, which are linked with several straits, and Larantuka Strait is one of them [see Fig. 3 (a) and the red box in Fig. 1 (b)]. This model aims to produce a valid surface elevation model in the domain. To obtain a valid tidal current velocity model, a more detailed mesh resolution is required. In order to optimize the computational time, a valid and detailed current velocity model is developed using the local model, which only covers Larantuka Strait, as shown in Fig. 3 (b) and Fig. 1 (b) (red box).

The model applies both offline and online nesting. Offline nesting is performed in the transition from global model to local model. Henceforth the local model water level boundary condition is derived from the result of global model. Online nesting is shown with the mesh becoming finer in the area of interest in both models.

The maximum and minimum global model mesh resolutions are 2 km and 200 m, respectively. The grid becomes finer when moving away from the boundary at Savu Sea, Banda Sea, and Flores Sea and into the strait. The base map resulting from the bathymetric survey combined with a navigational chart map from the Indonesian navy were used. The web open application NaoTide was used to develop the tidal fluctuation as the boundary condition at the outer boundary of the global model.

Meanwhile, in the local model, the maximum and minimum mesh resolutions are 1 km and 40 m. The local model was employed to provide detailed the tidal current velocity model in Larantuka Strait, resulting in 11 layers of tidally induced current velocity. The 11 layers mentioned above comprise one blank spot layer covering the height of the ADCP and a distance of 80 cm above the ADCP and 10 layers of current velocity. This conforms to the ADCP 10 measurement cell.

5.3. Model Validation

Model validation is carried out by comparing the model output with the current velocity obtained from field measurements. Notably in hydrodynamic modeling, the two most common parameters for validation are the surface elevation and current velocity [20] [21]. The errors are calculated with a simple formula as shown in Eq. (4), where $\eta_{Numerical\ Model}$ is the value obtained from the numerical model and $\eta_{Field\ Measurement}$ is the value obtained from field measurement data.

$$Error = \frac{\left|\eta_{Numerical\ Model} - \eta_{Field\ Measurement}\right|}{Field\ Measurement\ Tidal\ Range} \quad (4)$$

5.3.1 Surface elevation validation

Surface elevation validation in the local model is performed at S1 (tidal field measurement) as shown in Fig. 2. The results of the numerical model are validated using 10-minute-interval surface data. The validation gives an error of 4.04%, which is considered to be a good validation, as illustrated in Fig. 4.

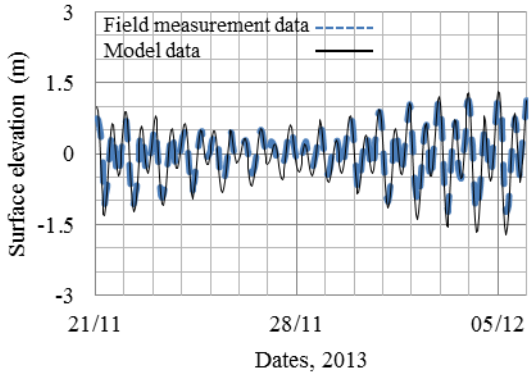

Fig.4 Surface elevation validation

5.3.2 Tidal current validation

Validation of the tidal current local model is carried out using field measurement data at locations S2 and S3 (see Fig. 2). The data are available in 10-minute intervals as well as a 10-layer composition, which gives a detail validation. Fig. 6 shows the validation.

The validation is carried out using both scatter plot of horizontal/vertical velocity and current magnitude time series. The scatter plot shows the correlation of model and field data current direction. Time series shows the agreement of current phase.

Table 1 shows the validation summary for each layer, and the average errors are 13.14 and 6.44% for S2 and S3 respectively. From the table it can be seen that the result of layer 5 gives the smallest error. As it is relatively far from the sea bed and ocean surface, the effects of both bed resistance and free surface waves do not interfere with the physical current. Layers 1, 2, 9, and 10 give large errors since they are close to the upper and bottom boundaries.

Table 1 Summary of tidal current validation error

Layer	Error S2 (%)	Error S3 (%)
1	14.74	7.48
2	13.82	6.69
3	13.23	6.31
4	13.05	6.18
5	12.60	5.99
6	12.68	6.11
7	12.75	6.17
8	12.78	6.27
9	12.60	6.77
Average	13.14	6.44

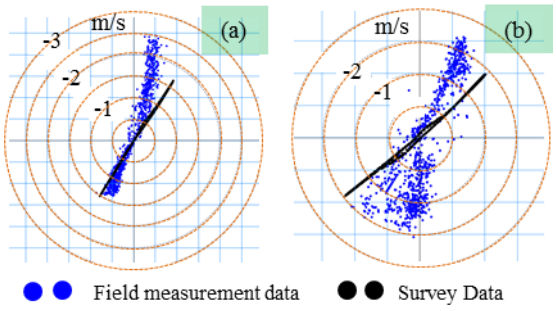

Fig.5 Validation of velocity using scatter plots at (a) S2 and (b) S3

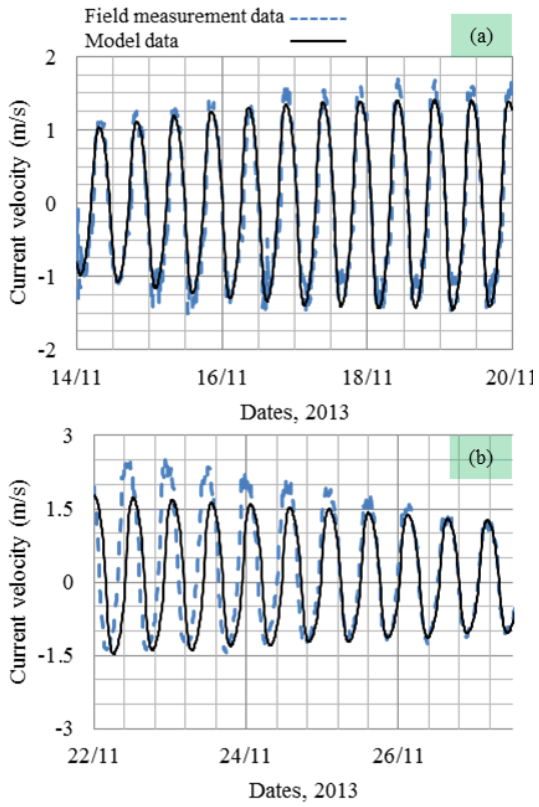

Fig. 6 Validation of time series velocity at (a) S2 and (b) S3

6. RESULTS AND ANALYSES

6.1 Tidal Current Model

Determination of a potential site for harvesting tide-induced power energy depends on the spatial and vertical distribution of the results of the numerical model of the tidal current.

The spatial distribution of the current velocity is extracted as the model result during spring flood, spring ebb, neap flood, and neap ebb, as seen in Fig. 7. The figures reveal that spring flood and neap flood conditions induce a larger magnitude of potential current velocity. As a result of the spatial distribution analysis, four points of interest are introduced, as seen in Fig. 8. The four locations are denoted by P1, P2, P3, and P4. Fig. 9 shows the scatter plot of tidal current velocity at each point. Location P2 is the best potential site.

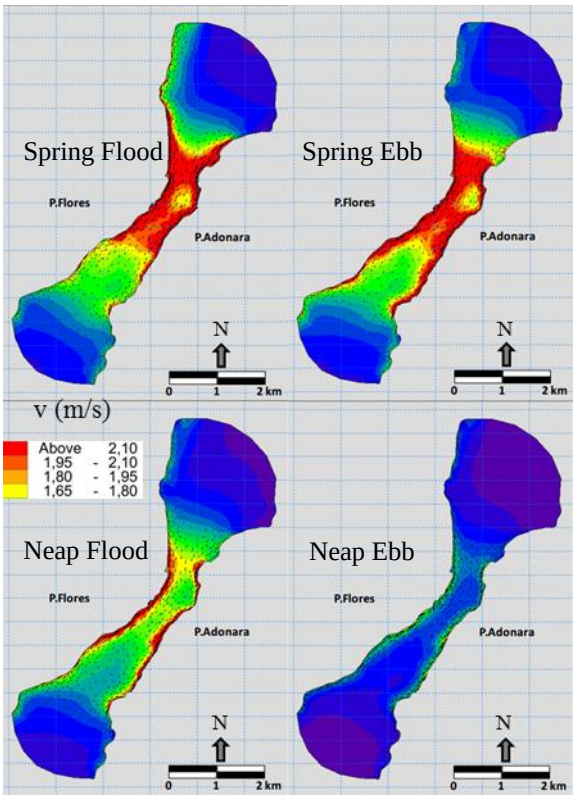

Fig.7 Spatial distributions of velocity under various conditions

As shown in Fig. 9 (b), the maximum velocity of P2 is approximately 2.5 m/s, which is five times higher than the maximum velocities of P1 and P4. The direction of the velocity shows good correlation with the geometry of the strait.

The vertical distributions of velocity under the spring flood condition in four cross-sections, A–A, B–B, C–C, and D–D, are shown in Fig. 10. Fig. 10

shows that the highest velocity is located in the uppermost layer. The tidal current velocity is above about 2.1 m/s in the majority of layers in sections B–B and C–C [see Fig. 10 (a,b)].

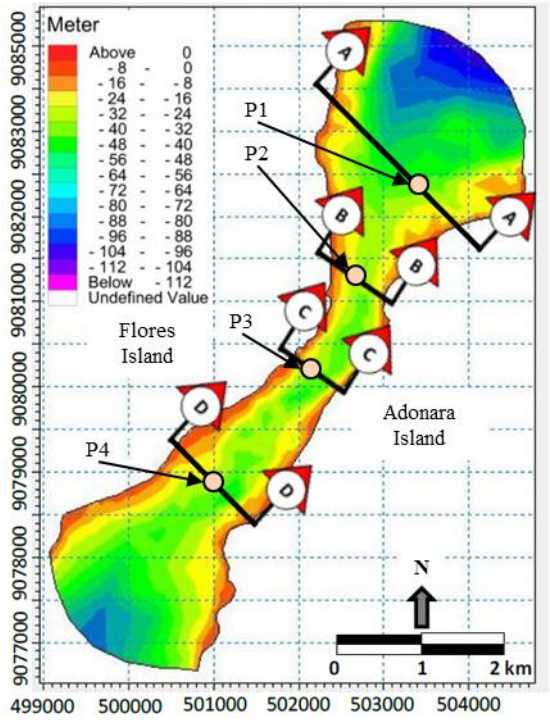

Fig.8 Locations and cross-sections of sites of interest

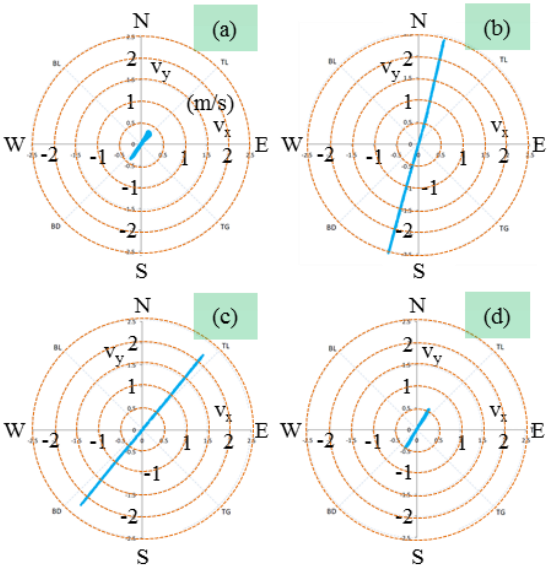

Fig. 9 Scatter plots of the sites of interest: (a) P1, (b) P2, (c) P3, and (d) P4

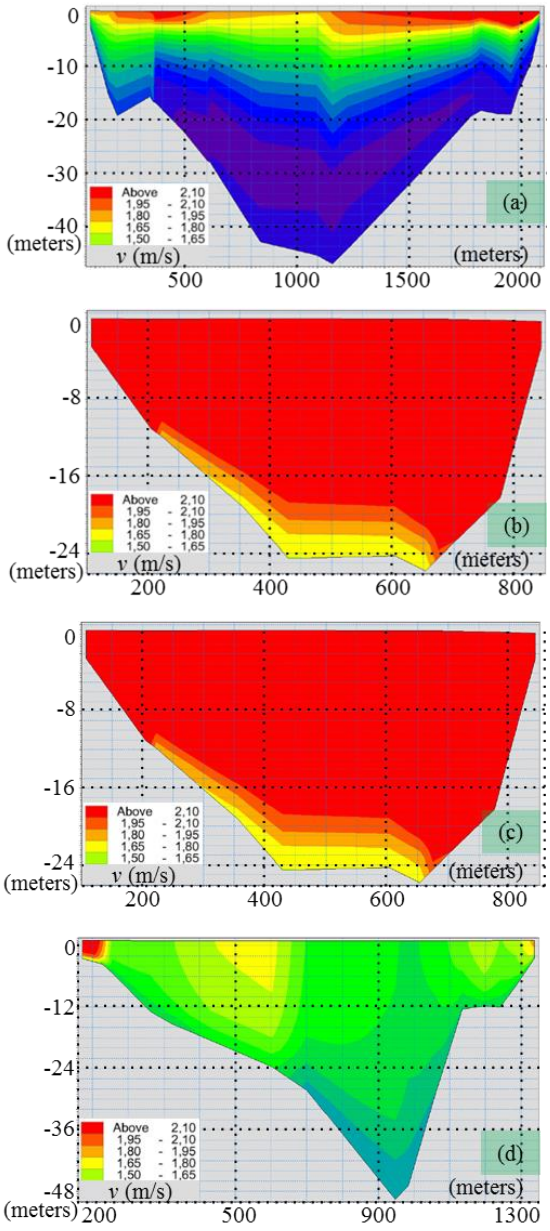

Fig.10 Cross-sections of velocity distribution of: (a) P1, (b) P2, (c) P3, and (d) P4.

By combining the analyses of both spatial and vertical distributions, it is found that the best potential location is around the middle of Larantuka Strait. The tapered geometrical shape of the strait causes a large tidal current velocity.

6.2 Power Calculation

The selected potential sites obtained from the model analysis of the tidal current are sites P2 and P3, with maximum velocities of around 2.5 and 2.3 m/s, respectively. Site P2 is named Larantuka1 and site P3 is named Larantuka2.

This study selects a Sabella turbine with a cut-in speed and a rated speed of 0.5 and 4 m/s, respectively [22]. The specific turbine type chosen is the D10 Sabella turbine. The D10 Sabella turbine is illustrated in Fig. 11. Such a turbine was installed near Ushant Island in 2015.

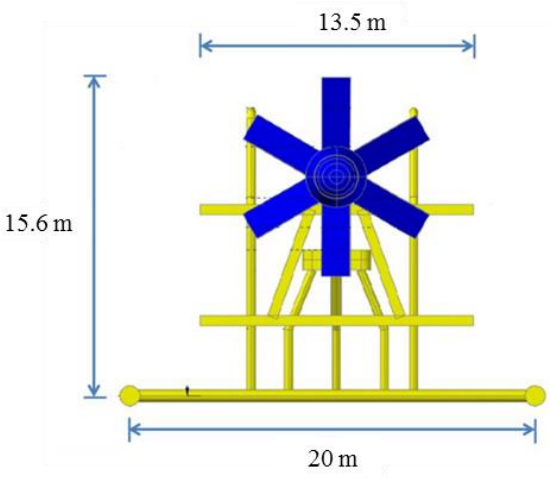

Fig.11 Illustration of D10 Sabella turbine

The power calculation is performed using Eq. (5):

$$\boldsymbol{E = \frac{1}{2} \times \rho \times \eta \times A \times v^3} \quad (5)$$

where E is the extracted power, ρ is the fluid density (1025 kg/m^3), η is the system efficiency, A is the turbine swept area (78.54 m^2), v is the tidal current velocity, and E_i is the power for the ith layer. The covered area needs to be considered thoroughly since the layers change dynamically with fluctuation of the water level. The considered layers are those that are covered by the turbine area, as given in Table 3. The total power is the sum of the power from the turbine-covered layers, as illustrated in Eq. 6. The power calculation is conducted for 365 days in 2014. The obtained extracted powers are presented in Table 3.

$$E = \frac{1}{2} \times \rho \times \eta \times A \times v^3 \quad (5)$$

$$E = E_1 + E_2 + ... + E_i \quad (6)$$

Using Eq. (5) with the time series velocity data at the two potential sites, the mean extracted power values in a year using a Sabella turbine at Larantuka1 and Larantuka2 are calculated to be 0.0597 and 0.037 MW, respectively. The extracted power in energy consumption units is 522.972 MWh at Larantuka1 and 324.12 MWh at Larantuka2 in 2014.

Table 2 D10 Efficiency of Sabella turbine

Efficiency type	Efficiency (%)
Turbine	50
Drive train	96
Generator	95
Power conditioning	98
Overall system	44.69

7. CONCLUSION

Larantuka Strait has been simulated successfully using a MIKE 3 hydrodynamic model in this study. The model closely represents the field data, with the errors in surface elevation and tidal current validation being 4.04 and 9.79%, respectively.

The result of this study are also in agreement with the findings of previous study. The tidal current at the middle of the strait has a powerful velocity of around 2.5 m/s at depths of about 20 to 30 m. Based on the analysis of the tidal current velocity model, the extracted power is calculated at two potential sites. The result shows that the amounts of generated electricity are 522.972 and 324.12 MWh using a D10 Sabella turbine.

Larantuka Strait is also found to be a very promising location, with a reasonable tidal current velocity speed and water depth, to install a tidal current turbine. To realize the vision of generating renewable energy in Larantuka Strait, it is strongly recommended that geotechnical, environmental, and sedimentation studies be performed. For a complete feasibility description of tidal current energy in Larantuka Strait, it is important to consider ship collision analysis and financial analysis too.

ACKNOWLEDGEMENT

The authors would like to thank the Ministry of Marine Affairs and Fisheries of the Republic of Indonesia for funding this research.

AUTHOR'S CONTRIBUTIONS

Author 1: Conception, design, field data acquisition, model and power calculation verification. **Author 2:** Field data acquisition and modeling. **Author 3:** Assist modeling, conduct power calculation and prepared manuscript. **Author 4:** Conception and model verification.

ETHICS

This article is original and contains unpublished material. The corresponding author confirms that all of the other authors have read and approved the manuscript and no ethical issues involved. This

article is original work and not under consideration for publication in any other journal. There are not conflict interest on this paper.

REFERENCES

[1] Murray RO, Gallego A, "A modelling study of the tidal stream resource of the Pentland Firth, Scotland", Renewable Energy, Vol. 102, 2017, pp. 326–340.

[2] Coles DS, Blunden LS, Bahaj AS, "Assessment of the energy extraction potential at tidal sites around the Channel Islands", Energy, Vol. 124, 2017, pp. 171–186.

[3] Karsten RH, McMillan JM, Lickley MJ, Haynes RD, "Assessment of tidal current energy in the Minas Passage, Bay of Fundy", Journal of Power and Energy, Vol. 222, 2008, pp. 493–507.

[4] Work PA, Haas KA, Defne Z, Gay T, "Tidal stream energy site assessment via three-dimensional model and measurements", Applied Energy, Vol. 102, 2013, pp. 510–519.

[5] Almeida MM, Cirano M, Soares CG, Lessa GC, "A numerical tidal stream energy assessment study for Baía de Todos os Santos, Brazil", Renewable Energy, Vol. 107, 2017, pp. 271–287.

[6] Gao P, Zheng J, Zhang J, Zhang T, "Potential assessment of tidal stream energy around Hulu Island, China", Procedia Engineering, Vol. 116, 2015, pp. 871–879.

[7] Tsai CH, Doong DJ, Chen YC, Yen CW, Maa MJ, "Tidal stream characteristics on the coast of Cape Fuguei in northwestern Taiwan for a potential power generation site", International Journal of Marine Energy, Vol. 13, 2016, pp. 193–205.

[8] Jo CH, Hwang SJ, Lee KH, "Tidal current energy resource assessment technique and procedure applied in western coastal region, South Korea", Journal of Energy and Power Engineering, Vol. 9, 2015, pp. 358–366.

[9] Novo PG, Kyozuka Y, "Field measurement and numerical study of tidal current turbulence intensity in the Kobe Strait of the Goto Islands, Nagasaki Prefecture", Journal of Marine Science and Technology, Vol. 22, 2016, pp. 335–350.

[10] Jeyaraj SK, Venugopal V, "Assessment of tidal energy potential along the Gulf of Khambhat, Gujarat, India.", Conf. Offshore Renewable Energy (CORE 2016), pp 1-6.

[11] Ihsan YN, Tussadiah A, Pridina N, Utamy RM, Astriandhita KM, Arnudin, Nurhasanah K, "Renewable energy from ocean currents on the outflow ITF pathway, Indonesia", Energy Procedia, Vol. 65, 2015, pp. 131–139.

[12] Orhan K, Mayerle R, Pandoe WW, "Assesment of energy production potential from tidal stream currents in Indonesia", Energy Procedia, Vol. 76, 2015, pp. 7–16.

[13] Blunden LS, Bahaj AS, Aziz NS, "Tidal current power for Indonesia? An initial resource estimation for the Alas Strait", Renewable Energy, Vol. 49, 2013, pp. 137–142.

[14] Rahman A, Venugopal V, "Parametric analysis of three dimensional flow models applied to tidal energy sites in Scotland", Estuarine, Coastal, and Shelf Science, Vol. 189, 2017, pp. 17–32.

[15] Pan Z, Liu H, "Numerical study of typhoon-induced storm surge in the Yangtze Estuary of China using a coupled 3D model", Procedia Engineering, Vol. 116, 2015, pp. 849–854.

[16] Morianou GG, Kourgialas NN, Karatzas GP, Nikolaidis NP, "Hydraulic and sediment transport simulation of Koiliaris River using the MIKE 21C model", Procedia Engineering, Vol. 162, 2016, pp. 463–470.

[17] Jia P, Wang Q, Lu X, Zhang B, Li C, Li S, Li S, Wang Y, "Simulation of the effect of an oil refining project on the water environment using the MIKE 21 model", Physics and Chemistry of the Earth, Parts A/B/C, accepted, 2017.

[18] Hartoko A, Helmi M, Sukarno M, Hariyado, "Spatial tsunami wave modeling for the South Java Coastal Area, Indonesia", International Journal of Geomate, Vol. 11, 2016, pp. 2455–2460.

[19] DHI Software, MIKE 21 & MIKE 3 Flow Model FM. Denmark: DHI Water & Environment, 2007, ch. 2. pp 10-12.

[20] Paboeuf S, Sun PYK, Macadre LM, Malgorn G, "Power performance assessment of tidal turbine Sabella D10 following IEC 62600-200", International Conference on Ocean, Offshore, and Arctic Engineering, 2016. pp 1-10.

[21] Hossain, M.Z. and Awal, A.S.M.A., Experimental validation of a theoretical model for flexural modulus of elasticity of thin cement composite, Construction and Building Materials, Vol. 25, No.3, pp.1460-1465, 2011.

[22] Bedard R, Previsic M, Siddiqui O, Hagerman G, Robinson M, Survey and Characterization — Tidal In Stream Energy Conversion (TISEC) Devices. EPRI-TP-004-NA, 2005. pp 168-178.